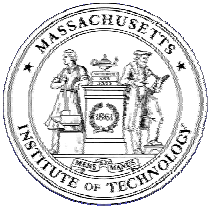


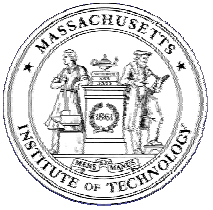
Computational Ocean Acoustics

- Ray Tracing
- Wavenumber Integration
- Normal Modes
- Parabolic Equation
- Broadband Modeling



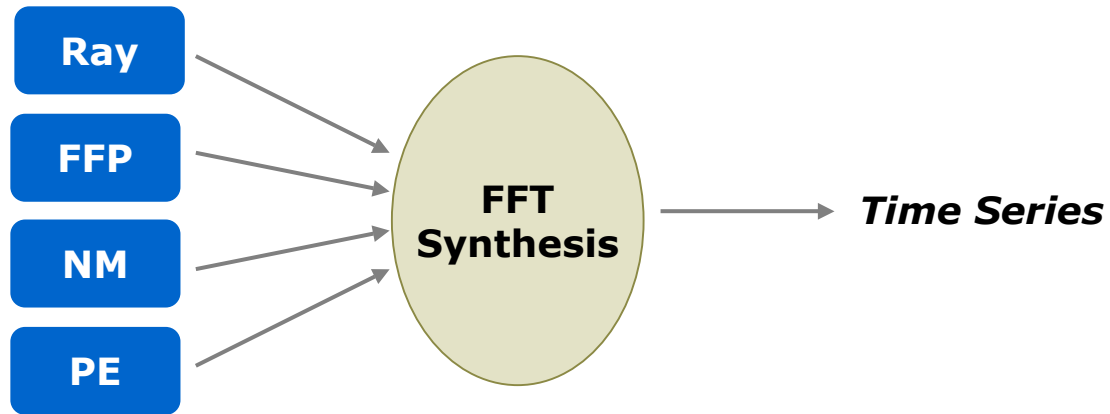
Broadband Modeling

- Fourier Synthesis
- Time-domain Methods
- Numerical Examples
- Doppler Shift in Ocean Waveguides
 - Numerical Examples



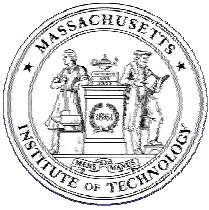
Broadband Modeling

Frequency Domain



Time Domain





Fourier Synthesis of Frequency-Domain Solutions

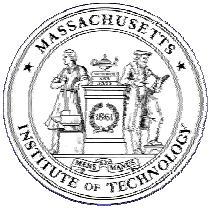
$$\begin{aligned} p(r, z, t) &= \frac{1}{2\pi} \int_{-\infty}^{\infty} p(r, z, \omega) e^{-i\omega t} d\omega \\ &= \frac{1}{2\pi} \int_{-\infty}^{\infty} S(\omega) g(r, z, \omega) e^{-i\omega t} d\omega, \end{aligned}$$

Frequency Windowing

$$p(r, z, t) = \frac{1}{2\pi} \int_{-\omega_{\max}}^{\omega_{\max}} S(\omega) \boxed{g(r, z, \omega)} e^{-i\omega t} d\omega.$$

Conjugate Symmetric
↙

$$p(r, z, t) = \operatorname{Re} \left\{ \frac{1}{\pi} \int_0^{\omega_{\max}} S(\omega) g(r, z, \omega) e^{-i\omega t} d\omega \right\}.$$



Fast Fourier Transforms

$$t_j = t_{\min} + j \Delta t, \quad j = 0, 1 \dots (N - 1),$$
$$\omega_\ell = \ell \Delta \omega, \quad \ell = -(N/2 - 1) \dots - 1, 0, 1 \dots (N/2 - 1),$$

FFT Sampling

$$\Delta t \Delta \omega = \frac{2\pi}{N}.$$

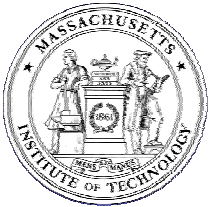
$$\Delta f = \frac{\Delta \omega}{2\pi} = \frac{1}{T}.$$

Periodicity

$$\sum_n p(r, z, t_j + nT) = \frac{\Delta \omega}{2\pi} \sum_{\ell=-(N/2-1)}^{N/2-1} [p(r, z, \omega_\ell) e^{-it_{\min}\omega_\ell}] e^{-i\frac{2\pi\ell j}{N}},$$

$$\sum_n p(r, z, t_j + nT) = \frac{\Delta \omega}{2\pi} \operatorname{Re} \left\{ \sum_{\ell=0}^{N/2-1} \epsilon_\ell [p(r, z, \omega_\ell) e^{-it_{\min}\omega_\ell}] e^{-i\frac{2\pi\ell j}{N}} \right\},$$

$$\epsilon_\ell = \begin{cases} 1 & \text{for } \ell = 0, \\ 2 & \text{for } \ell > 0. \end{cases}$$



Response in Time Window $[t_{\min}, t_{\min} + T]$

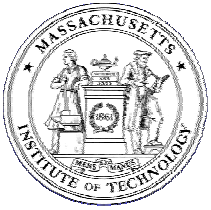
$$p(r, z, t_j) = \frac{\Delta\omega}{2\pi} \operatorname{Re} \left\{ \sum_{\ell=0}^{N/2-1} \epsilon_{\ell} [p(r, z, \omega_{\ell}) e^{-it_{\min}\omega_{\ell}}] e^{-i\frac{2\pi\ell j}{N}} \right\} \\ - \sum_{n \neq 0} p(r, z, t_j + nT),$$

$$\frac{N\Delta\omega}{2} > \omega_{\max},$$

$$\frac{N\Delta f}{2} > f_{\max}.$$

Nyquist Sampling Criterion

$$f_s = \frac{1}{\Delta t} > 2f_{\max}.$$



Time Windowing and Sampling

$$t_{\min} \leq \frac{r}{c_{\max}}$$

Reduced Time - Running Time Window

$$t' = t - r/c_{\max}$$

$$T = t_{\max} - t_{\min} \geq r_{\max} \left[\frac{1}{u_{\min}} - \frac{1}{c_{\max}} \right]$$

← Slowest arrival

← Fastest possible

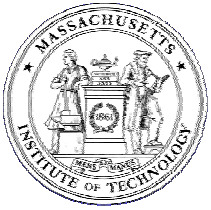
'Graphical' Sampling Requirement

$$\Delta t = \frac{T}{N} < \frac{1}{8f_{\max}}$$

Complex Frequency Integration

$$p(r, z, t_j) \simeq \frac{\Delta\omega}{2\pi} e^{\delta t_j} \operatorname{Re} \left\{ \sum_{\ell=0}^{N-1} \epsilon_{\ell} [p(r, z, \omega_{\ell} + i\delta) e^{-it_{\min}\omega_{\ell}}] e^{-i\frac{2\pi\ell j}{N}} \right\}$$

$$- \sum_{n \neq 0} p(r, z, t_j + nT) e^{-\delta nT}.$$



Attenuation and Causality

Plane Wave

$$p(0, t) = P\delta(t);$$

$$p(x, t) = \frac{1}{2\pi} \int_{-\infty}^{\infty} P e^{j\frac{\omega}{c}x - \alpha x} e^{-j\omega t} d\omega$$

Causality

$$p(x, t) = 0, \quad t < x/c;$$

Hilbert Transform

$$R(\omega) = \frac{1}{\pi} \int_{-\infty}^{\infty} \frac{I(y)}{\omega - y} dy$$

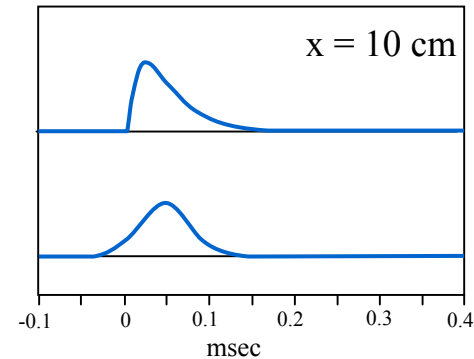
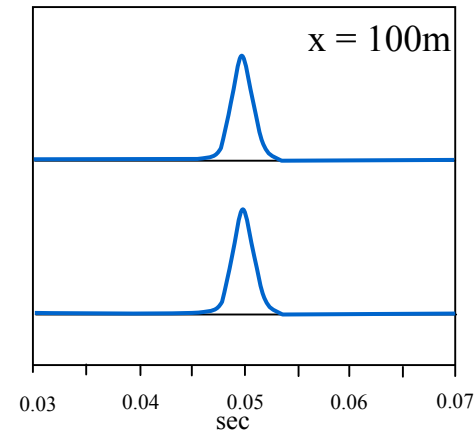
$$I(\omega) = \frac{1}{\pi} \int_{-\infty}^{\infty} \frac{R(y)}{\omega - y} dy$$

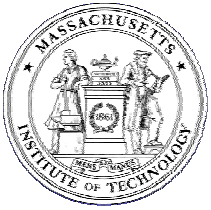
Plane Wave Solution

$$R(\omega) = e^{-\alpha(\omega)x} \cos(\omega x/c)$$

$$I(\omega) = e^{-\alpha(\omega)x} \sin(\omega x/c)$$

$$\Rightarrow c = c(\omega)$$





Attenuation and Causality

Plane Wave

$$p(0, t) = P\delta(t);$$

$$p(x, t) = \frac{1}{2\pi} \int_{-\infty}^{\infty} P e^{j\frac{\omega}{c}x - \alpha x} e^{-j\omega t} d\omega$$

Causality

$$p(x, t) = 0, \quad t < x/c;$$

Hilbert Transform

$$R(\omega) = \frac{1}{\pi} \int_{-\infty}^{\infty} \frac{I(y)}{\omega - y} dy$$

$$I(\omega) = \frac{1}{\pi} \int_{-\infty}^{\infty} \frac{R(y)}{\omega - y} dy$$

Plane Wave Solution

$$R(\omega) = e^{-\alpha(\omega)x} \cos(\omega x/c)$$

$$I(\omega) = e^{-\alpha(\omega)x} \sin(\omega x/c)$$

$$\Rightarrow c = c(\omega)$$

Causal Dispersion - Futterman

$$\alpha = \begin{cases} 0 & |\omega| < \omega_0 \\ b|\omega| & |\omega| > \omega_0 \end{cases}$$

$$\frac{1}{c(\omega)} = \frac{1}{c_0(\omega)} - \frac{b}{\pi} \log \left| \frac{\omega^2}{\omega_0^2} - 1 \right|$$

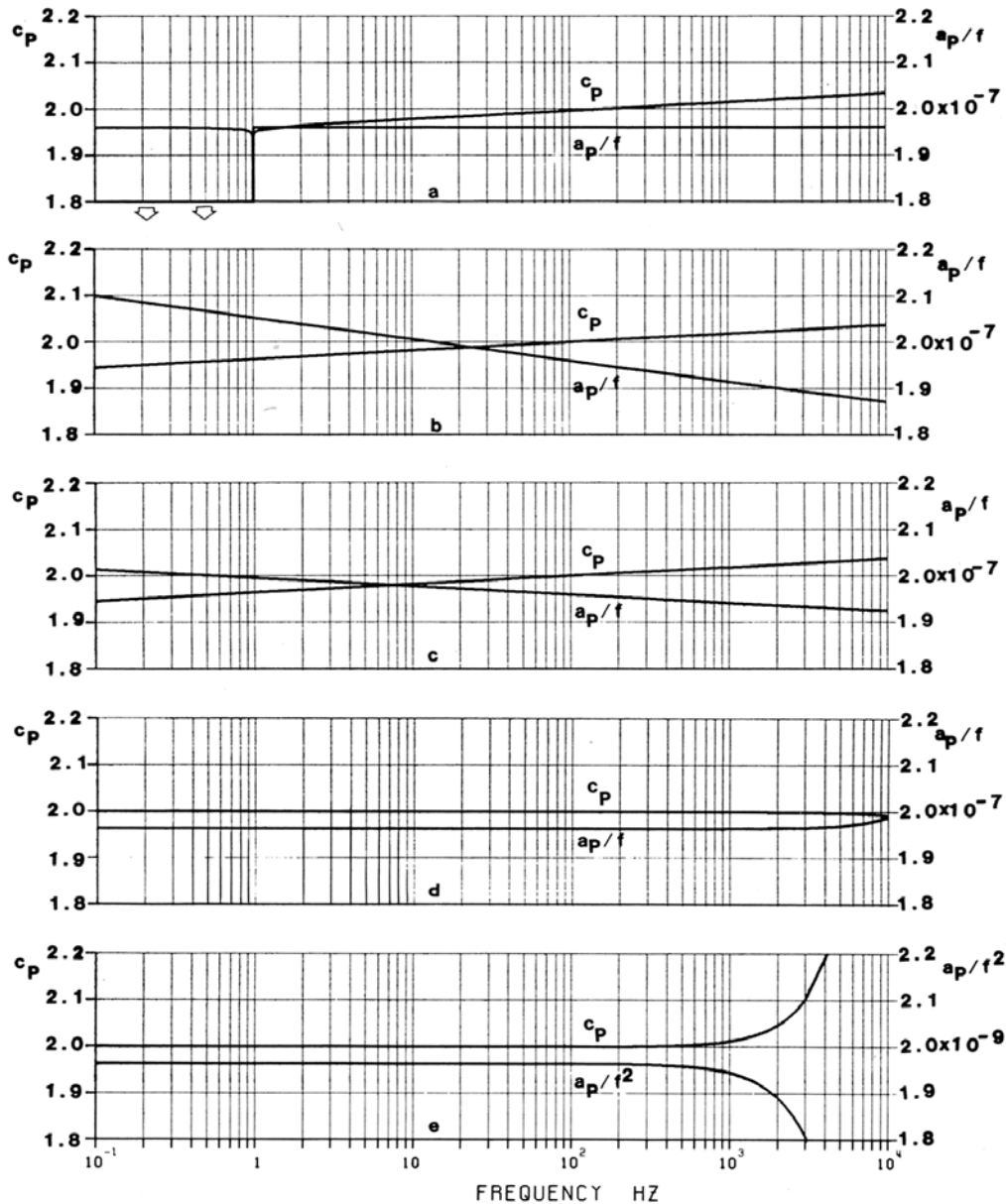
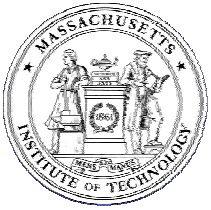
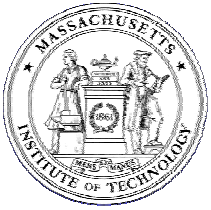


Fig. 4.25. Five attenuation–dispersion pairs: (a) truncated linear frequency; (b) power law attenuation; (c) Kjartansson model; (d) lumped-element model; (e) Voigt solid.

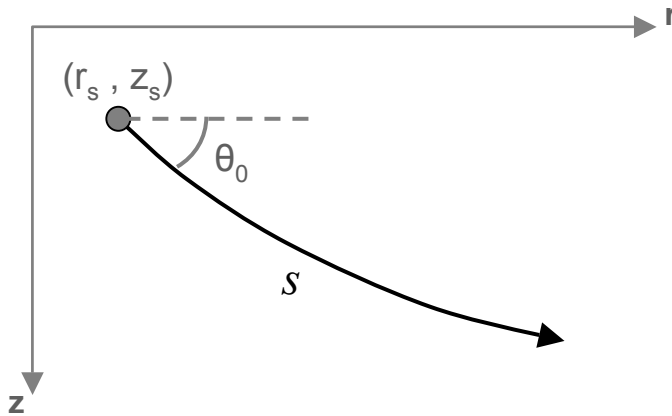
White, J.E. Figure 4.25 from *Underground sound: application of seismic waves*. Amsterdam; New York: Elsevier, 1983. Courtesy of Courtenay White. Used with permission.



Time-Domain Solutions

Ray Methods

Single Eigenray Contribution



$$p(s) = A(s) e^{i\omega\tau(s)},$$

$$\tau(s) = \int_0^s \frac{1}{c(s')} ds'.$$

Fourier Synthesis

$$p(s, t) = \frac{1}{2\pi} \int_{-\infty}^{\infty} S(\omega) p(s, \omega) e^{-i\omega t} d\omega,$$

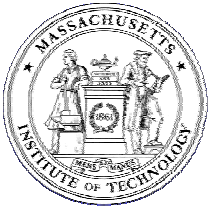
$$p(s, t) = A(s) \frac{1}{2\pi} \int_{-\infty}^{\infty} S(\omega) e^{-i\omega[t-\tau(s)]} d\omega.$$

$$p[s, t + \tau(s)] = A(s) \frac{1}{2\pi} \int_{-\infty}^{\infty} S(\omega) e^{-i\omega t} d\omega.$$

Time-delayed Source
Replica

$$p[s, t + \tau(s)] = A(s) S(t),$$

$$p(s, t) = A(s) S[t - \tau(s)].$$



Spectral Integral Techniques

Wave Equation in Cylindrical Coordinates

$$\rho \nabla \cdot \left(\frac{1}{\rho} \nabla p \right) - \frac{1}{c^2(z)} \frac{\partial^2 p}{\partial t^2} = -\frac{S(t)}{r} \delta(z - z_s, r),$$

Ideal Boundary Conditions

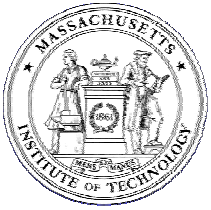
$$p(r, 0, t) = 0, \quad p_z(r, D, t) = 0.$$

$$p(r, z, t) \text{ outgoing as } r \rightarrow \infty.$$

$$p(r, z, 0) = p_t(r, z, 0) = 0.$$

Hankel Transform in Range

$$p(k_r, z, t) = \int_0^\infty p(r, z, t) J_0(k_r r) r dr,$$



Time-domain FFP

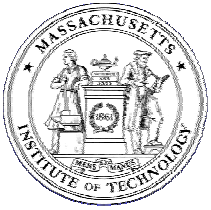
$$\left[\rho \frac{\partial}{\partial z} \left(\frac{1}{\rho} \frac{\partial}{\partial z} \right) - k_r^2 - \frac{1}{c^2(z)} \frac{\partial^2}{\partial t^2} \right] p(k_r, z, t) = -S(t) \delta(z - z_s),$$

$$p(k_r, 0, t) = 0,$$

$$p_z(k_r, D, t) = 0,$$

$$p(k_r, z, 0) = p_t(k_r, z, 0) = 0.$$

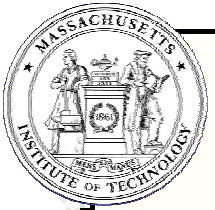
$$p(r, z, t) = \int_0^\infty p(k_r, z, t) J_0(k_r r) k_r dk_r.$$



Spherical wave incident on half-space: *direct, reflected, transmitted, and head/lateral/conical waves*

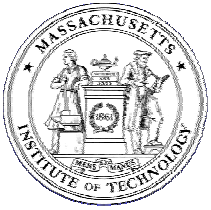
$$S(t) = \begin{cases} \sin(\omega_c t) - \frac{1}{2} \sin(2\omega_c t) & \text{for } 0 < t < 1/f_c \\ 0 & \text{else} \end{cases} .$$

[See Fig 8.2 in Jensen, Kuperman,
Porter and Schmidt. *Computational Ocean
Acoustics*. New York: Springer-Verlag, 2000.]



Spherical wave incident on a halfspace





Mode Dispersion in a Waveguide

Modal Group Velocity

$$u_m = \frac{d\omega}{dk_m},$$

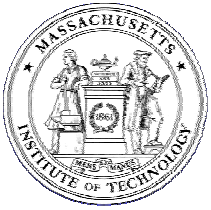
Modal Cutoff Frequency

$$f_{0m} = \frac{(m - 0.5) c_w}{2D\sqrt{1 - (c_w/c_b)^2}}.$$

Source Signal

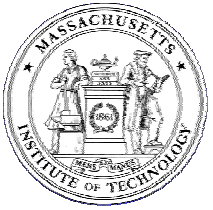
$$S(t) = \begin{cases} \frac{1}{2} \sin \omega_c t (1 - \cos \frac{1}{4} \omega_c t) & \text{for } 0 < t < 4/f_c \\ 0 & \text{else} \end{cases},$$

[See Jensen Fig 8.5]

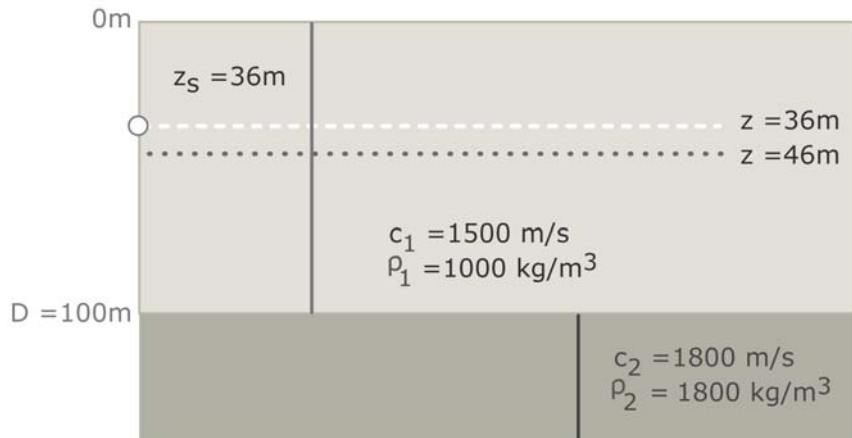


$$S(t) = \begin{cases} \frac{1}{2} \sin \omega_c t (1 - \cos \frac{1}{4} \omega_c t) & \text{for } 0 < t < 4/f_c \\ 0 & \text{else} \end{cases},$$

[See Jensen Fig 8.6, 8.7, 8.8]

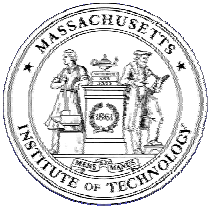


Shallow Water Waveguide with Fast Shear Bottom

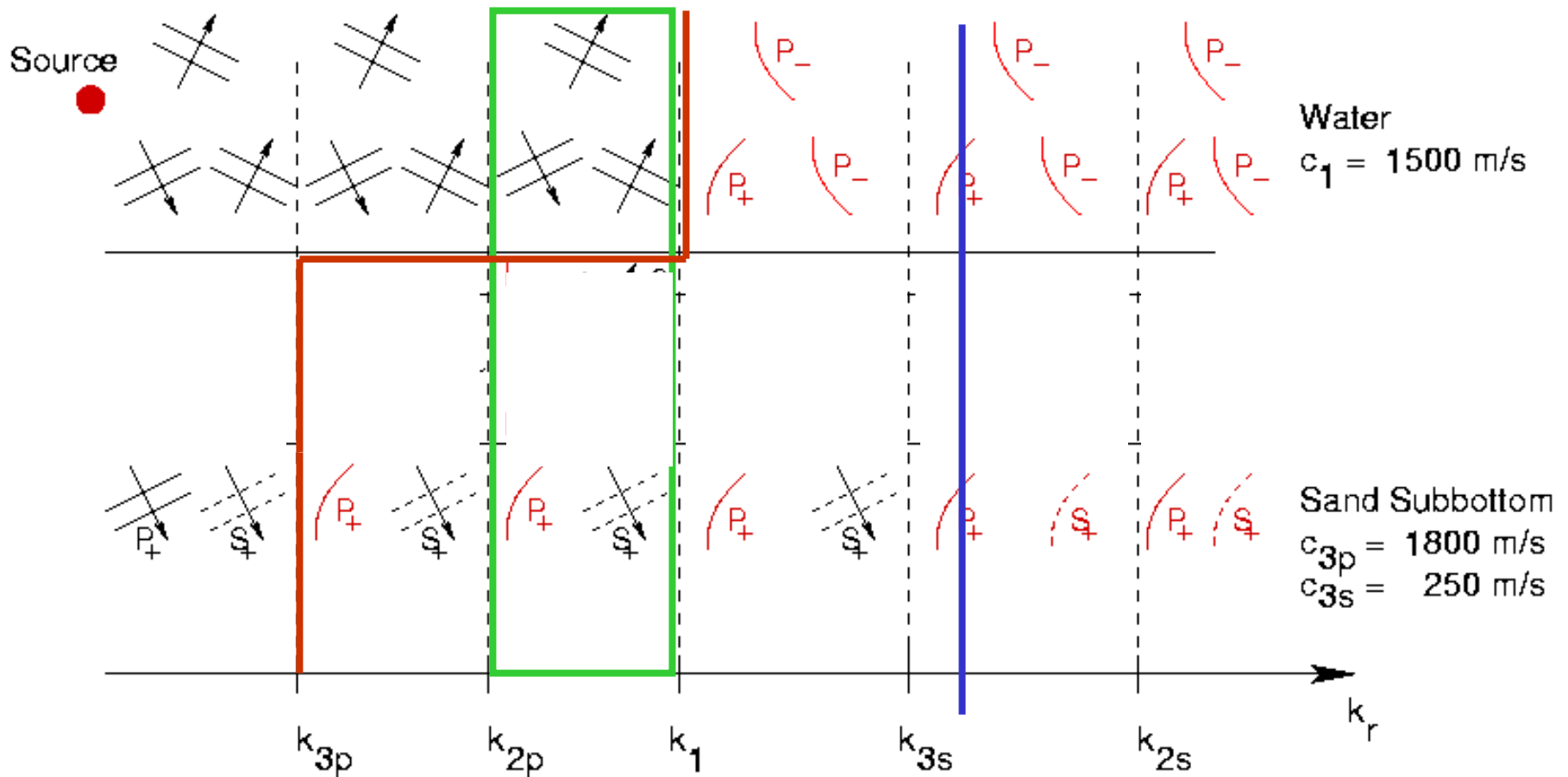


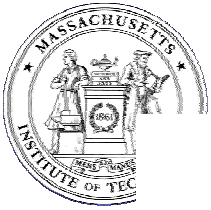
[See Jensen, Fig 4.9]

$$C_s = 600 \text{ m/s}$$



Stratified Elastic Bottom Scholte wave – Fast Sand Seabed





Scholte Waves in Shallow Water

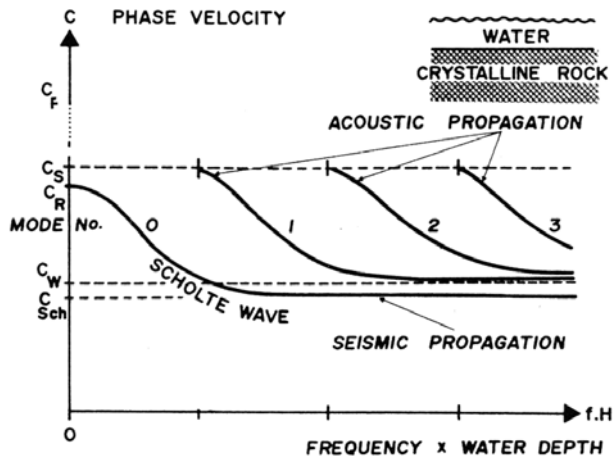


Fig. 1 Phase-velocities of the lowest modes in shallow water over an extremely "hard" rock-bottom

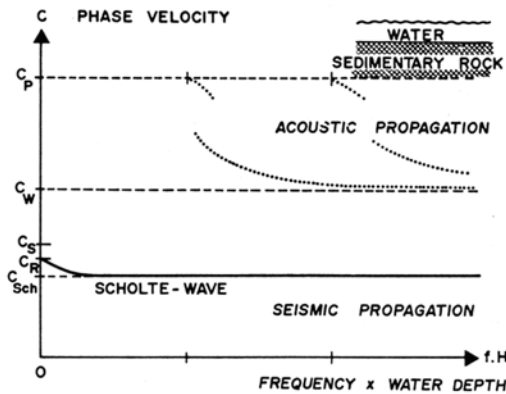


Fig. 2 Phase-velocities of the lowest modes in shallow water over a relative "soft" rock-bottom

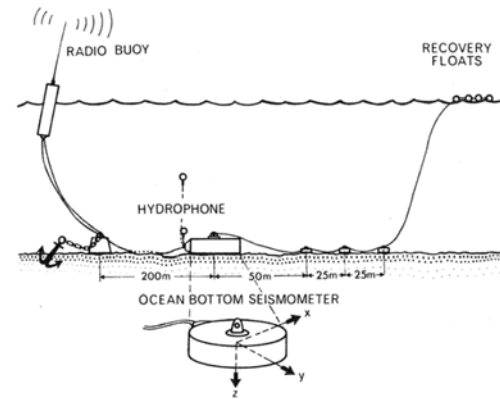


Fig. 8 Installation of the sensor package on the sea floor and mooring of its radio buoy in shallow water

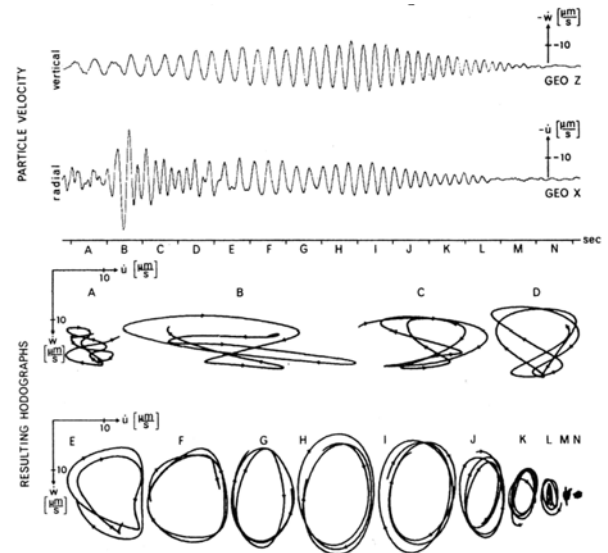
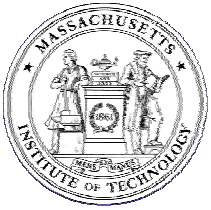


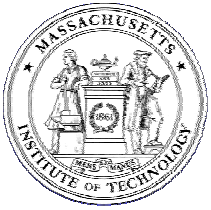
Fig. 12 Radial and vertical particle velocity of the interface wavelet in Fig. 11 with the resulting hodographs

Reproduced by permission from Rauch, Dieter, "Experimental and Theoretical Studies of Seismic Interface Waves in Coastal Waters." In *Bottom-Interacting Ocean Acoustics: NATO Conference Series, Marine Sciences*. Edited by William A. Kuperman & Finn B. Jensen. New York: Plenum Press, 1980.



Seismic Interface Waves

[See Jensen Figs. 8.9, 8.10, 8.11, 8.12]

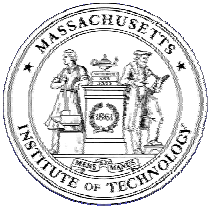


Seabed Shear Properties from Scholte Wave Inversions

Table 1 Interface wave experiments

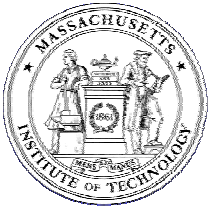
Investigators	Year	Water depth (m)	Bottom type	Centre freq. (Hz)	Measured att. (dB/km)	Inferred shear speed (m/s)	Inferred shear att. (dB/ λ_s)
Bucker, Whitney, Keir ⁶	1964	1 20	sand sand	20 25	300 200	100 195	1.4 1.4
Davies ⁷	1965	4410	-	6	-	50-190	-
Herron, Dorman, Drake ⁸	1968	5	silt	5	-	40-115	-
Hamilton et al. ⁹	1970	390 985	silt silt	- -	- -	100 90	- -
Schirmer ¹⁰	1980	130	sand	4.5	7	120	0.2
McDaniel, Beebe ¹¹	1980	32	sand	10	-	200	-
Essen et al. ¹²	1981	1	silt	4	-	75-250	-
Tuthill et al. ¹³	1981	7	mud	4.5	-	25-50	-
Whitmarsh, Lilwall ¹⁴	1982	5260	-	4.5	-	25-170	-
Holt, Hovem, Syrstad ¹⁵	1983	-	sand	35	600	135-195	2.3
Brocher et al. ¹⁶	1983	67	sand	5	0.43	260	0.02
Schmalfeldt, Rauch ¹⁷	1983	20 30	- -	3 3	10 2	100 150	0.3 0.1

Reproduced by permission from Jensen, Finn B. and Henrick Schmidt. "Shear Properties of Ocean Sediments Determined from Numerical Modelling of Scholte Wave Data." In Ocean Seismo-acoustics: Low Frequency Underwater Acoustics (NATO Conference Series, Marine Sciences). Edited by Tuncay Akal and Jonathan M. Berkson. New York: Plenum Press, 1986.



Deep-Water Propagation

[See Jensen Figs. 8.14, 8.15]



Deep-Water Propagation

Surface-Duct Propagation with Leakage

[See Jensen Figs. 8.16, 8.17]